



# CHORUS

This is the accepted manuscript made available via CHORUS. The article has been published as:

## Parity violation in radiative neutron capture on the deuteron

Young-Ho Song, Rimantas Lazauskas, and Vladimir Gudkov

Phys. Rev. C **86**, 045502 — Published 11 October 2012

DOI: [10.1103/PhysRevC.86.045502](https://doi.org/10.1103/PhysRevC.86.045502)

# Parity violation in radiative neutron capture on deuteron

Young-Ho Song,<sup>1,\*</sup> Rimantas Lazauskas,<sup>2,†</sup> and Vladimir Gudkov<sup>1,‡</sup>

<sup>1</sup>*Department of Physics and Astronomy,*

*University of South Carolina, Columbia, SC, 29208*

<sup>2</sup>*IPHC, IN2P3-CNRS/Université Louis Pasteur BP 28,*

*F-67037 Strasbourg Cedex 2, France*

(Dated: September 20, 2012)

## Abstract

Parity violating (PV) effects in neutron-deuteron radiative capture are studied using Desplanques, Donoghue, and Holstein (DDH) and effective field theory (EFT) weak potentials. The values of PV effects are calculated using wave functions, obtained by solving three-body Faddeev equations in configuration space for realistic strong potentials. The relations between physical observables and low-energy constants are presented, and dependencies of the calculated PV effects on strong and weak potentials are discussed. The presented analysis shows the possible reason for the existing discrepancy in PV nuclear data analysis using the DDH approach and reveals a new opportunity to study short range interactions in nuclei.

PACS numbers: 24.80.+y, 25.10.+s, 11.30.Er, 13.75.Cs

---

\*song25@mailbox.sc.edu

†rimantas.lazauskas@ires.in2p3.fr

‡gudkov@sc.edu

## I. INTRODUCTION

Low energy parity violating (PV) effects play an important role in understanding the main features of the Standard model. Many nuclear PV effects were measured and calculated during the last several years. Despite the fact that existing calculations of nuclear PV effects are in a reasonably good agreement with the measured ones, lately it became clear (see, for example [1–4] and references therein) that it is rather difficult to describe the available experimental data with the same set of weak nucleon coupling constants using the traditional DDH [5] weak meson exchange potential.

As a possible solution for this problem, a new approach, based on the effective field theory (EFT), has been introduced to parameterize PV effects in a model independent way (see, papers [1, 4, 6] and references therein). The main goal of the EFT approach is to describe a large number of PV effects in terms of a small number of constants (LEC), which are the free parameters of the theory. Unfortunately, the number of experimentally measured (and independent in terms of unknown LECs) PV effects in two body systems is not enough to constrain all LECs [7–10]. In order to determine these constants, it is necessary to include also the data obtained on heavier nuclear systems.

Furthermore, one should better understand PV effects in heavier nuclei because these effects might be essentially enhanced [11–13] in many body systems. However, how to apply the EFT approach for the calculations of PV effects in nuclei is still an open question.

To verify the possible issues related to the application of the DDH description of PV effects in nuclei and the possibility of systematic calculations of PV effects in nuclei using the EFT approach, it is desirable to start from the calculations of PV effects in the simplest nuclear systems, such as neutron-deuteron (n-d) compound. PV effects for elastic n-d scattering have been calculated recently [14, 15] using both the DDH and the EFT approaches. However, before extending these techniques to many-body nuclear systems, it is important to consider inelastic processes which are usually more sensitive to short range interactions.

With this aim, we present in this paper a comprehensive analysis of PV effects in neutron-deuteron radiative capture [16–19] using weak potential of the DDH-type, as well as weak potentials obtained in pionless and pionful EFT with realistic strong potential models. This “hybrid” method has an advantage to treat the DDH and the EFT approaches in the same framework. For strong interactions, we have tested several realistic nucleon-nucleon poten-

tials, also in conjunction with three-nucleon forces. Three-nucleon wave functions have been obtained by solving Faddeev equations in configuration space for the complete Hamiltonians comprising both weak and strong interactions.

The paper is structured as follows. In the next section, a brief description of the employed formalism is presented. Then, we discuss the results of our calculations and perform a detailed analysis of model and cutoff dependencies of the calculated PV parameters. In conclusion, the implications of our results are summarized.

## II. FORMALISM

We consider three parity violating observables in the radiative neutron capture on deuterons ( $n+d \rightarrow {}^3H + \gamma$ ) at thermal neutron energy: circular polarization of emitted photons ( $P^\gamma$ ), asymmetry of photons in relation to neutron polarization ( $a_n^\gamma$ ), and asymmetry of photons in relation to deuteron polarization ( $A_d^\gamma$ ). For low energy neutrons, the expressions for these PV effects could be written in terms of parity conserving magnetic dipole ( $M1$ ) and parity violating electric dipole ( $E1$ ) transition matrix elements as:

$$\begin{aligned}
a_n^\gamma &= \frac{2}{3} \frac{\text{Re} \left[ \sqrt{2}(E1_{\frac{3}{2}}^* M1_{\frac{1}{2}} + E1_{\frac{1}{2}}^* M1_{\frac{3}{2}}) + \frac{5}{2}(E1_{\frac{3}{2}}^* M1_{\frac{3}{2}}) - (E1_{\frac{1}{2}}^{*,(+)} M1_{\frac{1}{2}}) \right]}{|M1_{\frac{1}{2}}|^2 + |M1_{\frac{3}{2}}|^2}, \\
P^\gamma &= \frac{2\text{Re} \left[ E1_{\frac{1}{2}}^* M1_{\frac{1}{2}} + E1_{\frac{3}{2}}^* M1_{\frac{3}{2}} \right]}{|M1_{\frac{1}{2}}|^2 + |M1_{\frac{3}{2}}|^2}, \\
A_d^\gamma &= -\frac{\text{Re} \left[ -5E1_{\frac{3}{2}}^* M1_{\frac{3}{2}} - 4E1_{\frac{1}{2}}^* M1_{\frac{1}{2}} + \sqrt{2}E1_{\frac{3}{2}}^* M1_{\frac{1}{2}} + \sqrt{2}E1_{\frac{1}{2}}^* M1_{\frac{3}{2}} \right]}{2(|M1_{\frac{1}{2}}|^2 + |M1_{\frac{3}{2}}|^2)}. \tag{1}
\end{aligned}$$

Here,  $M1$  and  $E1$  amplitudes are defined as reduced matrix elements of the multipole operators

$$X1_J \equiv \langle -\mathbf{q}, J_B || \hat{T}_1^X || J \rangle, \quad \text{with } X = (M, E), \tag{2}$$

where  $J_B$  and  $J$  are total angular momenta of a bound and scattering states respectively, and  $\mathbf{q}$  is a momentum of the outgoing photon. The electromagnetic multipole operators in the limit of small  $q$  can be written as

$$\begin{aligned}
\hat{T}_{JM}^{Mag}(q) &\simeq -\frac{q^J}{i(2J+1)!!} \sqrt{\frac{J+1}{J}} \int d\mathbf{x} [\hat{\mu}(\mathbf{x}) + \frac{1}{J+1} \mathbf{r} \times \hat{\mathbf{J}}_c(x)] \cdot \nabla (x^J Y_{JM}) \\
\hat{T}_{JM}^{El}(q) &\simeq \frac{q^J}{(2J+1)!!} \sqrt{\frac{J+1}{J}} \int d\mathbf{x} (x^J Y_{JM} \hat{\rho}(x) - \frac{iq}{J+1} \hat{\mu}(x) \cdot [\mathbf{r} \times \nabla x^J Y_{JM}]),
\end{aligned}$$

where  $\hat{J}_c(x)$  is a convection current,  $\hat{\mu}(x)$  is a magnetization current,  $\hat{\rho}(x)$  is a charge operator, and  $q = \omega$  is a photon energy. In our calculations, we use the  $M1$  operator up to  $N^3LO$  in chiral order counting, which includes contributions from two-pion exchange and contact currents obtained in heavy baryon chiral perturbation theory [20]. For calculations of E1 amplitudes at the leading order, we use only the E1 charge operator, which is related to 3-vector currents by Siegert's theorem. Since in the used spherical harmonics convention both parity conserving  $M1$  and parity violating  $E1$  amplitudes are purely imaginary, it is convenient to define real-valued  $\widetilde{\mathcal{M}}_J$  and  $\widetilde{\mathcal{E}}_J$  matrix elements as

$$M1_J = i \frac{\omega \mu_N}{\sqrt{6\pi} \sqrt{4\pi}} \widetilde{\mathcal{M}}_J, \quad E1_J = -i \frac{\omega}{\sqrt{6\pi}} \widetilde{\mathcal{E}}_J, \quad (3)$$

where  $\mu_N = \frac{1}{2m_N}$ .

The results of calculations of parity conserving  $M1$  amplitudes for radiative thermal neutron capture on deuteron have been reported in papers [20, 21] using a ‘‘hybrid’’ method, where wave functions were obtained from realistic potential models and the current operators were derived from the heavy baryon chiral effective field theory. The results of these calculations can be approximated [20] by the following expressions <sup>1</sup>

$$\begin{aligned} \widetilde{\mathcal{M}}_{\frac{1}{2}} &= +21.87 + 10.76[(B_{model}/B_{exp})^{-2.5} - 1] \text{ fm}^{\frac{3}{2}}, \\ \widetilde{\mathcal{M}}_{\frac{3}{2}} &= -12.24 - 11.35[(B_{model}/B_{exp})^{-2.5} - 1] \text{ fm}^{\frac{3}{2}}, \end{aligned} \quad (4)$$

where two low energy constants of the two-body  $M1$  operators are fixed [20] by experimental values of  ${}^3H$  and  ${}^3He$  magnetic moments. In these expressions,  $M1$  amplitudes and the binding energy  $B_{model}$  of  ${}^3H$  depend on the model of strong interactions. However, the observed explicit correlation between the calculated  $M1$  amplitudes and the binding energy  $B_{model}$  provides the unique opportunity to eliminate this model dependence. This might be done by setting  $B_{model}/B_{exp} = 1$  in eq.(4). Then obtained  $M1$  amplitudes lead to the value of the total neutron-deuteron radiative capture cross section  $\sigma_{tot} = 0.49(1)$  mb, which is well consistent with the experimental data.

E1 amplitudes are calculated using three-body wave functions, which are obtained by solving Faddeev equations in a configuration space. We have tested different combinations

---

<sup>1</sup> The sign of the  $M1$  operator is changed from the one used in [20] to be consistent with the convention used in this work.

of strong and weak potentials. For a strong (parity conserving) part of the Hamiltonian, we choose a set of realistic models of nucleon-nucleon interactions, namely: Argonne v18 potential (AV18) [22], INOY potential [23], Reid soft-core potential (Reid) and Nijmegen potential(NijmII) [24]. Also, we have performed calculations for the AV18 potential in conjunction with the Urbana IX three-nucleon force potential [25] (denoted as AV18+UIX). In this paper, we consider three types of parity violating weak potentials: the standard DDH potential with meson exchange nucleon-nucleon interactions, the potential derived from pionless version, and the potential derived from pionful version of the effective field theory. Therefore, for the parity violating part of the Hamiltonian, we used one of these weak potentials and treated it as a perturbation to the parity conserving part of the Hamiltonian. Our approach could be considered as a “hybrid” method, similar to the “hybrid” approach in the line of Weinberg’s scheme [26, 27], which has been successfully applied for the calculations of weak and electromagnetic processes involving three-body and four-body hadronic systems [20, 21, 28–31], and for the calculations of parity violating [15] and time reversal violating effects in elastic n-d scattering [32, 33]. It is worth mentioning that alternative calculations of parity violating effects in elastic n-d scattering using pionless EFT [34] are well consistent with the hybrid calculations [15], though more detailed comparison between these two methods is required.

### A. The parity violating potentials

To understand the possible difference in the description of parity violating effects by the DDH and the EFT-type of potentials, we compare the operator structure of the potentials for the DDH potential [35] and for two different choices of the EFT potentials [1], which are derived from pionless and pionful EFT Lagrangian. All these potentials can be expanded in terms of  $O_{ij}^{(n)}$  operators [14] as

$$v_{ij}^{\alpha} = \sum_n c_n^{\alpha} O_{ij}^{(n)}, \quad \alpha = \text{DDH, pionless EFT or pionful EFT} \quad (5)$$

with the explicit forms for the operators  $O_{ij}^{(n)}$  and the corresponding parameters  $c_n^{\alpha}$ , listed in table I <sup>2</sup>, where coefficients  $c_n^{\alpha}$  have dimension of [fm] and scalar functions  $f_n^{\alpha}(r)$  have

---

<sup>2</sup> Note that we use a consistent relation between the coefficient  $C_6^{\not{x}}$  in a weak Lagrangian [14] and the coefficient  $c_1^{\not{x}}$  of a weak potential, which is different from the relation used in [15],  $c_1^{\not{x}} = \frac{2\mu^2}{\Lambda^3} C_6^{\not{x}}$ . However,

TABLE I: Parameters and operators of parity violating potentials.  $g_A = 1.26$ ,  $F_\pi = 92.4$  MeV.

$\mathcal{T}_{ij} \equiv (3\tau_i^z \tau_j^z - \tau_i \cdot \tau_j)$ . Scalar function  $\tilde{L}_\Lambda(r) \equiv 3L_\Lambda(r) - H_\Lambda(r)$ .

$n$	$c_n^{DDH}$	$f_n^{DDH}(r)$	$c_n^\pi$	$f_n^\pi(r)$	$c_n^\pi$	$f_n^\pi(r)$	$O_{ij}^{(n)}$
1	$+\frac{g_\pi}{2\sqrt{2}m_N}h_\pi^1$	$f_\pi(r)$	$-\frac{\mu^2 C_6^\pi}{\Lambda_\chi^3}$	$f_\mu^\pi(r)$	$+\frac{g_\pi}{2\sqrt{2}m_N}h_\pi^1$	$f_\Lambda^\pi(r)$	$(\tau_i \times \tau_j)^z (\boldsymbol{\sigma}_i + \boldsymbol{\sigma}_j) \cdot \mathbf{X}_{ij,-}^{(1)}$
2	$-\frac{g_\rho}{m_N}h_\rho^0$	$f_\rho(r)$	0	0	0	0	$(\tau_i \cdot \tau_j) (\boldsymbol{\sigma}_i - \boldsymbol{\sigma}_j) \cdot \mathbf{X}_{ij,+}^{(2)}$
3	$-\frac{g_\rho(1+\kappa_\rho)}{m_N}h_\rho^0$	$f_\rho(r)$	0	0	0	0	$(\tau_i \cdot \tau_j) (\boldsymbol{\sigma}_i \times \boldsymbol{\sigma}_j) \cdot \mathbf{X}_{ij,-}^{(3)}$
4	$-\frac{g_\rho}{2m_N}h_\rho^1$	$f_\rho(r)$	$\frac{\mu^2}{\Lambda_\chi^3}(C_2^\pi + C_4^\pi)$	$f_\mu^\pi(r)$	$\frac{\Lambda^2}{\Lambda_\chi^3}(C_2^\pi + C_4^\pi)$	$f_\Lambda(r)$	$(\tau_i + \tau_j)^z (\boldsymbol{\sigma}_i - \boldsymbol{\sigma}_j) \cdot \mathbf{X}_{ij,+}^{(4)}$
5	$-\frac{g_\rho(1+\kappa_\rho)}{2m_N}h_\rho^1$	$f_\rho(r)$	0	0	$\frac{2\sqrt{2}\pi g_A^3 \Lambda^2}{\Lambda_\chi^3}h_\pi^1$	$L_\Lambda^\pi(r)$	$(\tau_i + \tau_j)^z (\boldsymbol{\sigma}_i \times \boldsymbol{\sigma}_j) \cdot \mathbf{X}_{ij,-}^{(5)}$
6	$-\frac{g_\rho}{2\sqrt{6}m_N}h_\rho^2$	$f_\rho(r)$	$-\frac{2\mu^2}{\Lambda_\chi^3}C_5^\pi$	$f_\mu^\pi(r)$	$-\frac{2\Lambda^2}{\Lambda_\chi^3}C_5^\pi$	$f_\Lambda(r)$	$\mathcal{T}_{ij}(\boldsymbol{\sigma}_i - \boldsymbol{\sigma}_j) \cdot \mathbf{X}_{ij,+}^{(6)}$
7	$-\frac{g_\rho(1+\kappa_\rho)}{2\sqrt{6}m_N}h_\rho^2$	$f_\rho(r)$	0	0	0	0	$\mathcal{T}_{ij}(\boldsymbol{\sigma}_i \times \boldsymbol{\sigma}_j) \cdot \mathbf{X}_{ij,-}^{(7)}$
8	$-\frac{g_\omega}{m_N}h_\omega^0$	$f_\omega(r)$	$\frac{2\mu^2}{\Lambda_\chi^3}C_1^\pi$	$f_\mu^\pi(r)$	$\frac{2\Lambda^2}{\Lambda_\chi^3}C_1^\pi$	$f_\Lambda(r)$	$(\boldsymbol{\sigma}_i - \boldsymbol{\sigma}_j) \cdot \mathbf{X}_{ij,+}^{(8)}$
9	$-\frac{g_\omega(1+\kappa_\omega)}{m_N}h_\omega^0$	$f_\omega(r)$	$\frac{2\mu^2}{\Lambda_\chi^3}\tilde{C}_1^\pi$	$f_\mu^\pi(r)$	$\frac{2\Lambda^2}{\Lambda_\chi^3}\tilde{C}_1^\pi$	$f_\Lambda(r)$	$(\boldsymbol{\sigma}_i \times \boldsymbol{\sigma}_j) \cdot \mathbf{X}_{ij,-}^{(9)}$
10	$-\frac{g_\omega}{2m_N}h_\omega^1$	$f_\omega(r)$	0	0	0	0	$(\tau_i + \tau_j)^z (\boldsymbol{\sigma}_i - \boldsymbol{\sigma}_j) \cdot \mathbf{X}_{ij,+}^{(10)}$
11	$-\frac{g_\omega(1+\kappa_\omega)}{2m_N}h_\omega^1$	$f_\omega(r)$	0	0	0	0	$(\tau_i + \tau_j)^z (\boldsymbol{\sigma}_i \times \boldsymbol{\sigma}_j) \cdot \mathbf{X}_{ij,-}^{(11)}$
12	$-\frac{g_\omega h_\omega^1 - g_\rho h_\rho^1}{2m_N}$	$f_\rho(r)$	0	0	0	0	$(\tau_i - \tau_j)^z (\boldsymbol{\sigma}_i + \boldsymbol{\sigma}_j) \cdot \mathbf{X}_{ij,+}^{(12)}$
13	$-\frac{g_\rho}{2m_N}h_\rho^1$	$f_\rho(r)$	0	0	$-\frac{\sqrt{2}\pi g_A \Lambda^2}{\Lambda_\chi^3}h_\pi^1$	$L_\Lambda^\pi(r)$	$(\tau_i \times \tau_j)^z (\boldsymbol{\sigma}_i + \boldsymbol{\sigma}_j) \cdot \mathbf{X}_{ij,-}^{(13)}$
14	0	0	0	0	$\frac{2\Lambda^2}{\Lambda_\chi^3}C_6^\pi$	$f_\Lambda(r)$	$(\tau_i \times \tau_j)^z (\boldsymbol{\sigma}_i + \boldsymbol{\sigma}_j) \cdot \mathbf{X}_{ij,-}^{(14)}$
15	0	0	0	0	$\frac{\sqrt{2}\pi g_A^3 \Lambda^2}{\Lambda_\chi^3}h_\pi^1$	$\tilde{L}_\Lambda^\pi(r)$	$(\tau_i \times \tau_j)^z (\boldsymbol{\sigma}_i + \boldsymbol{\sigma}_j) \cdot \mathbf{X}_{ij,-}^{(15)}$

dimension of [fm<sup>-1</sup>].

The operators  $O_{ij}^{(n)}$  in the last column are represented as products of isospin, spin, and vector operators  $\mathbf{X}_{ij,\pm}^{(n)}$ , which are defined as

$$\begin{aligned} \mathbf{X}_{ij,+}^{(n)} &\equiv [\mathbf{p}_{ij}, f_n(r_{ij})]_+, \\ \mathbf{X}_{ij,-}^{(n)} &\equiv i[\mathbf{p}_{ij}, f_n(r_{ij})]_-, \end{aligned} \quad (6)$$

where  $\mathbf{p}_{ij} \equiv \frac{(\mathbf{p}_i - \mathbf{p}_j)}{2}$ .

One can see that all weak potentials have the same operator structure, being represented by fifteen symmetry allowed basic operators. Thus, the difference between weak potentials is

---

it does not affect our results in [15] because they are based only on the calculations of matrix elements of the  $O_{ij}^{(1)}$  operators.

TABLE II: The cutoff parameters for the DDH parity violating potentials in GeV units[36]. For the masses of the mesons we use  $m_\pi = 0.138$  GeV,  $m_\rho = 0.771$  GeV, and  $m_\omega = 0.783$  GeV.

	$\Lambda_\pi$	$\Lambda_\rho$	$\Lambda_\omega$
DDH-I	1.72	1.31	1.50
DDH-II	$\infty$	$\infty$	$\infty$

due merely to the choice of the coupling constants assigned to each operator and the scalar functions which describe the radial behavior of the term with a particular operator. The scalar functions in the DDH potential are constrained by the meson exchange mechanism. On the other hand, the scalar functions in the EFT potential are required to be only smooth and well localized functions. In this sense, the EFT potentials have more degrees of freedom than the DDH model, which assumes a specific meson-exchange dynamics.

For the case of the DDH potential, the radial functions  $f_x(r)$ ,  $x = \pi, \rho$ , and  $\omega$  are usually written as a normal or modified Yukawa functions with the corresponding cutoff terms

$$f_x(r) = \frac{1}{4\pi r} \left\{ e^{-m_x r} - e^{-\Lambda_x r} \left[ 1 + \frac{\Lambda_x r}{2} \left( 1 - \frac{m_x^2}{\Lambda_x^2} \right) \right] \right\}, \quad (7)$$

where,  $m_x$  is a  $x$ -meson mass, and  $\Lambda_x$  is the corresponding cutoff parameter. We adopt two sets of the scalar functions: with the cutoff terms (DDH-I) and without them (DDH-II), as described in Table II.

In the EFT, the results of calculations of low energy observables should be independent of specific forms of the scalar functions  $f_\mu(r)$  in the pionless EFT ( $\not{\pi}$ EFT) potentials and of the scalar functions, used for the contact terms, in pionful EFT ( $\pi$ EFT), provided these functions are well localized (close to the delta function) and, at the same time, are smooth enough to be used in numerical calculations. This is because the dependencies on the mass scale ( $\mu$ ) and on the particular choice of the form of these functions must be absorbed by the renormalization of the corresponding low energy constants. Thus, for our calculations in pionless EFT, we use two sets of the scalar functions, which we call  $\not{\pi}$ EFT-I and  $\not{\pi}$ EFT-II,

respectively <sup>3</sup>:

$$\begin{aligned} f_\mu(r) &= \frac{1}{4\pi r} e^{-\mu r}, \text{ for } \not\pi\text{EFT-I,} \\ f_\Lambda(r) &= \frac{1}{\Lambda^2} \delta_\Lambda(r) = \frac{1}{\Lambda^2} \int \frac{d^3 k}{(2\pi)^3} e^{-i\mathbf{k}\cdot\mathbf{r}} e^{-\frac{k^2}{\Lambda^2}}, \text{ for } \not\pi\text{EFT-II} \end{aligned} \quad (8)$$

with the mass scale parameters  $\mu$  and  $\Lambda$ , which provide a cutoff scale of the theory. For example, the natural scale of the cutoff parameters in pionless theory is  $(\mu, \Lambda) \simeq m_\pi$ .

The pionful EFT model ( $\pi$ EFT) has explicit long range interaction terms resulting from one pion exchange ( $V_{-1,LR}$ ) and from higher order long range corrections ( $V_{1,LR}$ ). Also, it has middle range interactions terms due to two pion exchange ( $V_{1,MR}$ ) contributions, as well as short range interactions ( $V_{1,SR}$ ) terms due to nucleon contact interactions. The radial part of the leading term of the long range one pion exchange,  $V_{-1,LR}$ , is described by the modified Yukawa function  $f_\pi(r)$ . The short range interaction function  $V_{1,SR}$  in the pionful theory has the same structure as in the pionless EFT. However, in spite of the structural similarity, the origin of these functions is different, therefore, as a consequence, their numerical values can be different. The only term in pionful EFT which has a different operator structure, in compare to the DDH and the pionless EFT potentials, is a higher order long range correction term  $V_{1,LR}^{PV}$ . We can ignore these higher order corrections related to long range interactions because they are suppressed and can be absorbed by the renormalization of low energy constants [6]. Therefore, the pionful EFT does not introduce a new operator structure as long as we neglect  $V_{1,LR}^{PV}$  term [6, 37]. The middle range interaction terms  $V_{1,MR}$  can be described by  $L(q)$  and  $H(q)$  functions in a momentum space

$$L(q) \equiv \frac{\sqrt{4m_\pi^2 + \mathbf{q}^2}}{|\mathbf{q}|} \ln \left( \frac{\sqrt{4m_\pi^2 + \mathbf{q}^2} + |\mathbf{q}|}{2m_\pi} \right), \quad H(q) \equiv \frac{4m_\pi^2}{4m_\pi^2 + \mathbf{q}^2} L(q), \quad (9)$$

where,  $q^\mu = (q^0, \mathbf{q}) = p_1^\mu - p_1'^\mu = p_2'^\mu - p_2^\mu$ . For the sake of simplicity, to transform these scalar functions into a configuration space representation by Fourier transform, we use only one cutoff parameter for all regulators  $S_\Lambda(q)$ . Therefore, one can write

$$\{L_\Lambda(r), H_\Lambda(r), f_\Lambda(r), f_\Lambda^\pi(r)\} = \frac{1}{\Lambda^2} \int \frac{d^3 q}{(2\pi)^3} e^{-i\mathbf{q}\cdot\mathbf{r}} S_\Lambda(q) \{L(q), H(q), 1, \frac{\Lambda^2}{\mathbf{q}^2 + m_\pi^2}\}, \quad (10)$$

where  $L_\Lambda(r)$  and  $H_\Lambda(r)$  correspond to two-pion exchange loop contributions,  $f_\Lambda(r)$  and  $f_\Lambda^\pi(r)$  describe short range contact terms and long range one-pion exchange contributions,

---

<sup>3</sup> Note that these functions are different from ones used in [15].

correspondingly. It should be noted that we introduce the cutoff function even for the case of a long range one-pion exchange potential to regularize a short range part of one-pion exchange. Among the possible choices, we use two types of regulators, which are called  $\pi$ EFT-I and  $\pi$ EFT-II<sup>4</sup>:

$$S_{\Lambda}^{exp}(\mathbf{q}) = e^{-\frac{\mathbf{q}^2}{\Lambda^2}} \text{ for } \pi\text{EFT-I}, \quad S_{\Lambda}^{dipole}(\mathbf{q}) = \frac{(\Lambda^2 - 4m_{\pi}^2)^2}{(\Lambda^2 + \mathbf{q}^2)^2} \text{ for } \pi\text{EFT-II}. \quad (11)$$

One can see that the function  $f_{\Lambda}(r)$  in the  $\pi$ EFT-I looks similar to the function for the  $\not{\pi}$ EFT-II case; however, it leads to different regularizations since a typical value of the cutoff parameter for the  $\pi$ EFT theory exceeds the pion mass scale and should be at least about of the  $\rho$  meson mass scale, while for the pionless case it is close to the pion mass. Therefore, the LECs for the same operators in the pionless and the pionful EFT potentials can be very different.

## B. Three nucleon wave functions

Nuclear wave functions of initial (neutron-deuteron scattering) and final (bound triton) states of the neutron-deuteron radiative capture process are obtained in the context of a non-relativistic quantum three particle problem. We consider neutrons and protons as an isospin degenerate states of the same particle nucleon, whose mass is fixed to  $\hbar^2/m = 41.471$  MeV·fm. The three-particle problem is formulated by means of Faddeev equations in a configuration space [38]. Using the isospin formalism, three Faddeev equations become formally identical, which for pairwise interactions reads

$$(E - H_0 - V_{ij}) \psi_k = V_{ij}(\psi_i + \psi_j), \quad (12)$$

where  $(ijk)$  are particle indexes,  $H_0$  is kinetic energy operator,  $V_{ij}$  is a two body force between particles  $i$ , and  $j$ ,  $\psi_k = \psi_{i,j,k}$  is so called Faddeev component. In the last equation, the potential formally contains both strong interaction, parity conserving, part ( $V_{ij}^{PC}$ ) and weak interaction, parity violating, part ( $V_{ij}^{PV}$ ), i.e.:  $V_{ij} = V_{ij}^{PC} + V_{ij}^{PV}$ . Due to the presence of a parity violating potential, the system's wave function does not have a definite parity and contains both positive and negative parity components. As a consequence, the Faddeev

---

<sup>4</sup> Note that the convention is different from the one used in [15].

components of the total wave function can be split into the sum of positive and negative parity parts:

$$\psi_k = \psi_k^+ + \psi_k^- \quad (13)$$

At low neutron energies, the dominant components of both initial and final state nuclear wave functions have positive parity. Parity violating interaction is weak ( $V_{ij}^{PV} \ll V_{ij}^{PC}$ ); then by neglecting second order weak potential terms, one obtains a system of two differential equations:

$$(E - H_0 - V_{ij}^{PC}) \psi_k^+ = V_{ij}^{PC}(\psi_i^+ + \psi_j^+), \quad (14)$$

$$(E - H_0 - V_{ij}^{PC}) \psi_k^- = V_{ij}^{PC}(\psi_i^- + \psi_j^-) + V_{ij}^{PV}(\psi_i^+ + \psi_j^+ + \psi_k^+) \quad (15)$$

One can see that the first equation (14) defines only the positive parity part of the wave function. This equation contains only a strong nuclear potential and corresponds to the standard three nucleon problem: s-wave neutron-deuteron scattering, or an bound state of the triton. The solution of the second differential equation (15), which contains inhomogeneous term  $V_{ij}^{PV}(\psi_i^+ + \psi_j^+ + \psi_k^+)$ , gives us negative parity components of wave functions.

To solve these equations numerically, we use our standard procedure, described in detail in [39]. Using a set of Jacobi coordinates, defined by  $\mathbf{x}_k = (\mathbf{r}_j - \mathbf{r}_i)$  and  $\mathbf{y}_k = \frac{2}{\sqrt{3}}(\mathbf{r}_k - \frac{\mathbf{r}_i + \mathbf{r}_j}{2})$ , we expand each Faddeev component of the wave function in bipolar harmonic basis:

$$\psi_k^\pm = \sum_\alpha \frac{F_\alpha^\pm(x_k, y_k)}{x_k y_k} \left| (l_x (s_i s_j)_{s_x})_{j_x} (l_y s_k)_{j_y} \right\rangle_{JM} \otimes |(t_i t_j)_{t_x} t_k\rangle_{TT_z}, \quad (16)$$

where index  $\alpha$  represents all allowed combinations of the quantum numbers presented in the brackets,  $l_x$  and  $l_y$  are the partial angular momenta associated with respective Jacobi coordinates,  $s_i$  and  $t_i$  are spins and isospins of the individual particles. Functions  $F_\alpha(x_k, y_k)$  are called partial Faddeev amplitudes. It should be noted that the total angular momentum  $J$ , as well as its projection  $M$ , are conserved. Isospin breaking is taken fully into account by considering both  $T = 1/2$  and  $T = 3/2$  channels of the total isospin.

Equations (14) and (15) must be supplemented with the appropriate boundary conditions for Faddeev partial amplitudes  $F_\alpha^\pm$ . First of all, partial Faddeev amplitudes are regular at the origin:

$$F_\alpha^\pm(0, y_k) = F_\alpha^\pm(x_k, 0) = 0. \quad (17)$$

For the bound state problem, the system's wave function also vanish exponentially as either  $x_k$  or  $y_k$  becomes large. This condition is imposed by setting Faddeev amplitudes to vanish

at the borders  $(x_{max}, y_{max})$  of a chosen grid , i.e.:

$$F_{\alpha}^{\pm}(x_k, y_{max}) = 0, \quad F_{\alpha}^{\pm}(x_{max}, y_k) = 0. \quad (18)$$

For neutron-deuteron scattering with energies below the break-up threshold, partial Faddeev amplitudes also vanish for  $\mathbf{x}_k \rightarrow \infty$ , thus the last equality in (18) also applies for the scattering.

At  $\mathbf{y}_k \rightarrow \infty$ , all Faddeev amplitudes vanish except for those consistent with the open channel, describing neutron-deuteron relative motion. For the case of thermal neutrons, we keep only relative s-wave amplitudes in the asymptote. This behavior is imposed by:

$$F_{\alpha}^{(\pm)}(x, y_{max}) = f_{l_x, j_x, s_x, t_x}^{(\pm)}(x) \left( y_{max} - \frac{2}{\sqrt{3}} a_J \right) \delta_{l_y, 0} \delta_{j_y, 1/2} \delta_{j_x, 1}. \quad (19)$$

Here,  $f_{l_x, j_x}^{(\pm)}(x)$  are reduced deuteron wave function components with respective parity  $(\pm)$ , orbital momentum  $l_x$ , total angular momentum  $j_x$ , total spin  $s_x$  and total isospin  $t_x$ . The corresponding deuteron wave function is calculated before three-nucleon scattering problem is undertaken. Neutron-deuteron scattering lengths  $a_J$  for the angular momenta  $J = 1/2$  and  $J = 3/2$  are obtained by solving equation (14).

The formalism described above can be easily generalized to accommodate three-nucleon forces, as is described in paper [40].

### C. Evaluation of the matrix elements

In order to calculate parity violating  $E1$  matrix elements, we define real  $\tilde{\mathcal{E}}_J^{(n)}$  matrix elements corresponding to each operator  $O^{(n)}$  as

$$\tilde{\mathcal{E}}_J = \sum_n c_n \tilde{\mathcal{E}}_J^{(n)}, \quad (20)$$

where the sum is taken over different parity violating operators with corresponding LECs  $c_n$ , defined in the Table I. At the leading order, the electromagnetic charge operator does not violate parity. Therefore, parity violating  $E1$  amplitude results only from a small admixture of parity violating components of wave functions. In the convention we use, parity violating wave functions are purely imaginary both for a bound state and for a zero energy n-d scattering; then one has

$$\tilde{\mathcal{E}}_J^{(n)} = -\tilde{\mathcal{E}}_{J,(+)}^{(n)} + \tilde{\mathcal{E}}_{J,(-)}^{(n)}, \quad (21)$$

where  $\tilde{\mathcal{E}}_{J,(\pm)}$  are amplitudes for transitions from a parity conserving scattering wave to a parity violating bound state, and from a parity violating scattering wave to a parity conserving bound state, respectively.

In the first order of perturbation, parity violating  $E1$  amplitudes can be presented as a linear combination of matrix elements  $X^{(m)}$  calculated for each of parity violating potential operators  $O_{ij}^{(m)}$ . Then, all PV observables  $a_n^\gamma$ ,  $P^\gamma$ ,  $A_d^\gamma$  can be expanded as

$$X = \sum \left( \frac{c_m}{\mu_N} \right) X^{(m)}, \quad (22)$$

(where  $X$  stands for  $a_n^\gamma$ ,  $P^\gamma$ , or  $A_d^\gamma$ , and  $\mu_N$  is introduced because of a dimension of coefficients  $c_m$ ) in terms of the corresponding multipole amplitudes  $X^{(m)}$ , presented by the following expressions:

$$a_n^{\gamma,(m)} = \left( -\frac{2}{3}\sqrt{4\pi} \right) \frac{\left[ \sqrt{2}(\tilde{\mathcal{E}}_{\frac{3}{2}}^{(m)} \tilde{\mathcal{M}}_{\frac{1}{2}} + \tilde{\mathcal{E}}_{\frac{1}{2}}^{(m)} \tilde{\mathcal{M}}_{\frac{3}{2}}) + \frac{5}{2}(\tilde{\mathcal{E}}_{\frac{3}{2}}^{(m)} \tilde{\mathcal{M}}_{\frac{3}{2}}) - (\tilde{\mathcal{E}}_{\frac{1}{2}}^{(m)} \tilde{\mathcal{M}}_{\frac{1}{2}}) \right]}{|\tilde{\mathcal{M}}_{\frac{1}{2}}|^2 + |\tilde{\mathcal{M}}_{\frac{3}{2}}|^2} \quad (23)$$

$$P^{\gamma,(m)} = \left( -2\sqrt{4\pi} \right) \frac{\left[ \tilde{\mathcal{E}}_{\frac{1}{2}}^{(m)} \tilde{\mathcal{M}}_{\frac{1}{2}} + \tilde{\mathcal{E}}_{\frac{3}{2}}^{(m)} \tilde{\mathcal{M}}_{\frac{3}{2}} \right]}{|\tilde{\mathcal{M}}_{\frac{1}{2}}|^2 + |\tilde{\mathcal{M}}_{\frac{3}{2}}|^2} \quad (24)$$

$$A_d^{\gamma,(m)} = \left( \frac{1}{2}\sqrt{4\pi} \right) \frac{\left[ -5\tilde{\mathcal{E}}_{\frac{3}{2}}^{(m)} \tilde{\mathcal{M}}_{\frac{3}{2}} - 4\tilde{\mathcal{E}}_{\frac{1}{2}}^{(m)} \tilde{\mathcal{M}}_{\frac{1}{2}} + \sqrt{2}\tilde{\mathcal{E}}_{\frac{3}{2}}^{(m)} \tilde{\mathcal{M}}_{\frac{1}{2}} + \sqrt{2}\tilde{\mathcal{E}}_{\frac{1}{2}}^{(m)} \tilde{\mathcal{M}}_{\frac{3}{2}} \right]}{(|\tilde{\mathcal{M}}_{\frac{1}{2}}|^2 + |\tilde{\mathcal{M}}_{\frac{3}{2}}|^2)}. \quad (25)$$

It should be noted that for the EFT potentials, each parity violating coefficient  $c_n$  has an explicit cutoff or scale dependence multiplier  $\frac{1}{\mu^2}$  (or  $\frac{1}{\Lambda^2}$ ). Therefore, we present all results in normalized forms, as  $\mu^2$ (or  $\Lambda^2$ )  $\times$   $\tilde{\mathcal{E}}^{(m)}$ (or  $X^{(n)}$ ), to remove this artificial scale dependence.

We calculate parity violating  $E1$  amplitude using one-body charge operator

$$E1_J = \langle J_B || \frac{q}{\sqrt{6\pi}} \sum_i Q_i r_i || J \rangle = (-i) \sum_n \frac{\omega}{\sqrt{6\pi}} c_n \tilde{\mathcal{E}}_J^{(n)}, \quad (26)$$

where,  $Q_i$  and  $r_i$  are  $i$ -th nucleons charge and the position in the center of mass system, such that

$$\sum_{i=1}^3 Q_i \mathbf{r}_i = \frac{1}{2} \left( \frac{1}{2} \mathbf{x}_3 (\tau_2 - \tau_1)^z + \frac{1}{\sqrt{3}} \mathbf{y}_3 \left( \tau_3 - \frac{\tau_1 + \tau_2}{2} \right)^z \right). \quad (27)$$

Then, using the wave function expansion

$$|\psi_i\rangle = \sum_\alpha \frac{F_{\alpha,i}(x,y)}{xy} |\alpha\rangle, \quad (28)$$

one obtains

$$\begin{aligned}
E1 = & \sqrt{\frac{1}{6\pi}}\omega\left(\sqrt{\frac{3}{4}}\right)^3 \sum_{\alpha,\beta} \int dx x^2 \int dy y^2 \left( \frac{F_{\beta,f}^*(x,y)}{xy} \frac{1}{4} x \frac{F_{\alpha,i}(x,y)}{xy} \langle \beta || \hat{x} || \alpha \rangle \langle \beta | (\tau_2 - \tau_1)^z | \alpha \rangle \right. \\
& \left. + \frac{F_{\beta,f}^*(x,y)}{xy} \frac{1}{2\sqrt{3}} y \frac{F_{\alpha,i}(x,y)}{xy} \langle \beta || \hat{y} || \alpha \rangle \langle \beta | \left( \tau_3 - \frac{\tau_1 + \tau_2}{2} \right)^z | \alpha \rangle \right), \tag{29}
\end{aligned}$$

where  $(\sqrt{\frac{3}{4}})^3$  comes from the normalization of  $y$ . The angular parts of these matrix elements are calculated analytically, while the radial integrals are taken numerically.

### III. RESULTS AND DISCUSSIONS

The results of our calculations are presented separately for the three choices of weak potentials: for the DDH potential, for the pionless and for the pionful potentials derived in the EFT approach.

#### A. The DDH potential results

The results obtained with the DDH potential are in a reasonably good agreement with the previous calculations [16–19], considering the difference in wave functions, and give us the opportunity to estimate the values of all PV effects in terms of PV meson-nucleon coupling constants  $h$  as

$$\begin{aligned}
a_n &= 0.42h_\pi^1 - 0.17h_\rho^0 + 0.085h_\rho^1 + 0.008h_\rho^2 - 0.238h_\omega^0 + 0.086h_\omega^1 - 0.010h_\rho^{\prime 1} = 4.11 \times 10^{-7} \tag{30} \\
P_\gamma &= -1.05h_\pi^1 + 0.19h_\rho^0 - 0.096h_\rho^1 - 0.018h_\rho^2 + 0.28h_\omega^0 - 0.046h_\omega^1 + 0.023h_\rho^{\prime 1} = -7.31 \times 10^{-7} \tag{31} \\
A_d^\gamma &= -1.51h_\pi^1 + 0.17h_\rho^0 - 0.083h_\rho^1 - 0.024h_\rho^2 + 0.024h_\omega^0 + 0.013h_\omega^1 + 0.032h_\rho^{\prime 1} = -9.05 \times 10^{-7} \tag{32}
\end{aligned}$$

The coefficients in these expressions are obtained using strong AV18+UIX and weak DDH-II potentials, while the final values of PV observables are given for the “best” values of the DDH coupling constants. The contributions of different PV operators to the transition amplitudes  $\tilde{\mathcal{E}}_{J,(P)}$ , where  $(P)$  indicates the parity of scattering waves, are shown in Table III. One can see that unlike the n-d elastic scattering case, there is no dominance of the  $J = \frac{3}{2}$  channel and, as a consequence, all operators contribute almost equally to the capture process.

TABLE III: Parity violating amplitudes  $\tilde{\mathcal{E}}_{J,(P)}$  in  $\text{fm}^{\frac{3}{2}}$  units, where  $(P)$  stands for the parity of a scattering wave, calculated with AV18+UIX strong and DDH-II weak potentials.

n	$\tilde{\mathcal{E}}_{\frac{1}{2},(+)}$	$\tilde{\mathcal{E}}_{\frac{1}{2},(-)}$	$\tilde{\mathcal{E}}_{\frac{3}{2},(+)}$	$\tilde{\mathcal{E}}_{\frac{3}{2},(-)}$
1	$-3.37 \times 10^{-1}$	$-3.75 \times 10^{-2}$	$-1.44 \times 10^{-2}$	$-2.97 \times 10^{-1}$
2	$-2.64 \times 10^{-3}$	$-1.52 \times 10^{-2}$	$-5.37 \times 10^{-3}$	$-2.52 \times 10^{-2}$
3	$-9.72 \times 10^{-3}$	$3.12 \times 10^{-2}$	$-1.35 \times 10^{-2}$	$1.31 \times 10^{-2}$
4	$1.03 \times 10^{-2}$	$-1.32 \times 10^{-2}$	$1.47 \times 10^{-2}$	$-2.87 \times 10^{-3}$
5	$1.26 \times 10^{-2}$	$-1.56 \times 10^{-2}$	$1.75 \times 10^{-2}$	$-3.79 \times 10^{-3}$
6	$-2.03 \times 10^{-3}$	$-8.85 \times 10^{-3}$	$-1.85 \times 10^{-3}$	$1.51 \times 10^{-3}$
7	$-2.42 \times 10^{-3}$	$-9.62 \times 10^{-3}$	$-2.45 \times 10^{-3}$	$1.94 \times 10^{-3}$
8	$-7.37 \times 10^{-3}$	$2.43 \times 10^{-2}$	$-1.08 \times 10^{-2}$	$9.51 \times 10^{-3}$
9	$-7.10 \times 10^{-3}$	$1.24 \times 10^{-2}$	$-1.05 \times 10^{-2}$	$-2.14 \times 10^{-3}$
10	$9.79 \times 10^{-3}$	$-1.25 \times 10^{-2}$	$1.39 \times 10^{-2}$	$-2.71 \times 10^{-3}$
11	$1.20 \times 10^{-2}$	$-1.48 \times 10^{-2}$	$1.67 \times 10^{-2}$	$-3.61 \times 10^{-3}$
12	$-2.75 \times 10^{-3}$	$9.29 \times 10^{-3}$	$-4.10 \times 10^{-4}$	$-9.10 \times 10^{-3}$
13	$-3.05 \times 10^{-3}$	$1.84 \times 10^{-2}$	$-1.96 \times 10^{-3}$	$-1.53 \times 10^{-2}$

TABLE IV: The DDH PV coupling constants in units of  $10^{-7}$  ( $h'_\rho$  contribution is neglected). The strong interactions parameters are  $\frac{g_\pi^2}{4\pi} = 13.9$ ,  $\frac{g_\rho^2}{4\pi} = 0.84$ ,  $\frac{g_\omega^2}{4\pi} = 20$ ,  $\kappa_\rho = 3.7$ , and  $\kappa_\omega = 0$ .

DDH Coupling	DDH ‘best’	4-parameter fit[41]
$h_\pi^1$	+4.56	-0.456
$h_\rho^0$	-11.4	-43.3
$h_\rho^2$	-9.5	37.1
$h_\omega^0$	-1.9	13.7
$h_\rho^1$	-0.19	-0.19
$h_\omega^1$	-1.14	-1.14

TABLE V: Parity violating observables for different potential models with the DDH-best parameter values and Bowman’s 4-parameter fits in  $10^{-7}$  units.

models	DDH-best values			4-parameter fits		
	$a_n$	$P_\gamma$	$A_d$	$a_n$	$P_\gamma$	$A_d$
AV18+UIX/DDH-I	3.30	-6.38	-8.23	1.97	-2.16	-1.81
AV18/DDH-II	4.61	-8.30	-10.3	4.60	-5.18	-4.46
AV18+UIX/DDH-II	4.11	-7.30	-9.04	4.14	-4.71	-4.09
Reid/DDH-II	4.74	-8.45	-10.4	4.70	-5.25	-4.46
NijmII/DDH-II	4.71	-8.45	-10.5	4.76	-5.26	-4.41
INOY/DDH-II	9.24	-12.9	-13.8	17.5	-17.9	-13.5

To check the possible model dependence of these results, we compare PV observables for the “best” DDH values and for the 4-parameter fit [41] of weak coupling constants (see Table IV). For weak potentials, we used both DDH-I and DDH-II radial functions with strong interactions described by AV18, AV18+UIX, Reid, NijmII, and INOY models. The results for these calculations are summarized in Table V. The difference in the values of  $P_\gamma$  and  $A_d$  effects for the “best” DDH values and for the 4-parameter fit proves that PV effects in radiative capture are very sensitive to the particular choice of the values of meson-nucleon coupling constants. The  $a_n$  observable is less sensitive to the choice of weak coupling constants for some strong potentials. However, since we do not know exact values of the weak coupling constants, we have to consider a model dependence of individual amplitudes rather than a total sum of them. These individual matrix elements are very sensitive to the choice of strong potentials as is discussed below. This model dependence indicates a possible serious problem in the calculation of PV effects in nuclei because many old calculations of PV effects in nuclei often used different potential models without a consistent treatment of model dependencies. A detailed discussion of the potential model dependencies is given in a later part of this paper.

## B. Pionless EFT potential results

Let us analyze the EFT approach with PV potentials obtained in the pionless EFT by using scalar functions corresponding to two different schemes for a cutoff procedure:  $\not\pi$ EFT-I and  $\not\pi$ EFT-II. The calculated PV amplitudes for these two weak EFT potentials with the same AV18+UIX strong interaction potential are summarized in Table VI. The difference between  $\not\pi$ EFT-I and  $\not\pi$ EFT-II results is not surprising because they have different forms of the scalar functions. A correct comparison of these two calculations should be done after the renormalization of all LECs for each case, however there is not enough experimental data to obtain these LECs. For further discussions of cutoff and model dependencies see a later section.

TABLE VI: Parity violating amplitudes  $\tilde{\mathcal{E}}_{J,(P)}$  for AV18+UIX strong interaction and PV  $\not\pi$ EFT-I and PV  $\not\pi$ EFT-II potentials with  $\mu = 138$  MeV.

op	$\not\pi$ EFT-I				$\not\pi$ EFT-II			
	$\tilde{\mathcal{E}}_{\frac{1}{2}(+)}$	$\tilde{\mathcal{E}}_{\frac{1}{2}(-)}$	$\tilde{\mathcal{E}}_{\frac{3}{2}(+)}$	$\tilde{\mathcal{E}}_{\frac{3}{2}(-)}$	$\tilde{\mathcal{E}}_{\frac{1}{2}(+)}$	$\tilde{\mathcal{E}}_{\frac{1}{2}(-)}$	$\tilde{\mathcal{E}}_{\frac{3}{2}(+)}$	$\tilde{\mathcal{E}}_{\frac{3}{2}(-)}$
1	-0.164	-0.0183	-0.00704	-0.145	-0.579	-0.766	0.0409	-0.136
4	0.268	-0.274	0.399	-0.0964	0.428	0.0462	0.681	0.157
6	-0.00616	-0.196	-0.0390	0.0530	0.0711	-0.179	-0.0555	-0.0291
8	-0.302	0.407	-0.297	0.218	-0.592	0.00657	-0.515	0.0643
9	-0.0863	0.174	-0.148	0.00634	-0.145	0.313	-0.316	0.139

The contributions of different operators from these two weak EFT potentials with the same AV18+UIX strong potential to PV effects are shown in Table VII. One can see that in the pionless EFT, all operators have approximately the same level of contribution to PV effects, which is consistent with the results for the DDH model.

TABLE VII: Parity violating observables for AV18+UIX strong potential for  $\not{\pi}$ EFT-I and  $\not{\pi}$ EFT-II at  $\mu = 138$  MeV. The results are in  $fm^{-2}$  units.

n	$\frac{c_n}{\mu_N \mu^2}$	$\not{\pi}$ EFT-I			$\not{\pi}$ EFT-II		
		$\mu^2 a_n^{(n)}$	$\mu^2 P_\gamma^{(n)}$	$\mu^2 A_d^{(n)}$	$\mu^2 a_n^{(n)}$	$\mu^2 P_\gamma^{(n)}$	$\mu^2 A_d^{(n)}$
1	$\frac{4m_N}{\Lambda_\chi^3} C_6^\not{\pi}$	0.0217	-0.0552	-0.0793	-0.0273	0.0216	0.00919
4	$\frac{2m_N}{\Lambda_\chi^3} (C_2^\not{\pi} + C_4^\not{\pi})$	-0.0794	0.0655	0.0316	-0.0556	0.0219	-0.0232
6	$-\frac{2}{\Lambda_\chi^3} C_r^\not{\pi}$	-0.0281	0.0596	0.0801	-0.0369	0.0653	0.0808
8	$-\frac{4m_N}{\Lambda_\chi^3} C_1^\not{\pi}$	0.104	-0.103	-0.0758	0.0875	-0.0676	-0.0262
9	$\frac{4m_N}{\Lambda_\chi^3} \widetilde{C}_1^\not{\pi}$	0.0381	-0.0429	-0.0367	0.0671	-0.0502	-0.0171

### C. Pionful EFT potential results

The PV transition amplitudes calculated for strong AV18+UIX potential and PV pionful EFT potential with cutoff parameter  $\Lambda = 600$  MeV are presented in Table VIII. The results for PV observables are provided in Table IX. It reveals a strong dependence on the choice of the scalar functions which, as is mentioned in the previous section, are expected to be absorbed by the corresponding LECs. (For the comparison with the pionless case, one shall take into account additional  $\Lambda^2/\Lambda_\chi^2$  multipliers in the coefficients of leading one-pion exchange operators which appear due to loop diagrams contributions in the pionful EFT.)

TABLE VIII: E1 amplitudes calculated for AV18+UIX and  $\pi$ EFT-I at  $\Lambda = 600$  MeV in  $\text{fm}^{\frac{3}{2}}$  unit. (The  $\Lambda^2$  multiplier is not included.)

operator	$\tilde{\mathcal{E}}_{\frac{1}{2}(+)}$	$\tilde{\mathcal{E}}_{\frac{1}{2}(-)}$	$\tilde{\mathcal{E}}_{\frac{3}{2}(+)}$	$\tilde{\mathcal{E}}_{\frac{3}{2}(-)}$
1	$-3.51 \times 10^{-1}$	$-7.40 \times 10^{-2}$	$-1.15 \times 10^{-2}$	$-2.86 \times 10^{-1}$
4	$3.56 \times 10^{-2}$	$-3.86 \times 10^{-2}$	$4.97 \times 10^{-2}$	$-7.90 \times 10^{-3}$
5	$3.43 \times 10^{-2}$	$-4.36 \times 10^{-2}$	$4.81 \times 10^{-2}$	$-9.25 \times 10^{-3}$
6	$-7.37 \times 10^{-3}$	$-3.18 \times 10^{-2}$	$-6.42 \times 10^{-3}$	$4.20 \times 10^{-3}$
8	$-2.65 \times 10^{-2}$	$7.65 \times 10^{-2}$	$-3.75 \times 10^{-2}$	$2.84 \times 10^{-2}$
9	$-2.32 \times 10^{-2}$	$4.48 \times 10^{-2}$	$-3.51 \times 10^{-2}$	$-5.06 \times 10^{-3}$
13	$-4.32 \times 10^{-4}$	$6.26 \times 10^{-2}$	$-6.46 \times 10^{-3}$	$-4.36 \times 10^{-2}$
14	$-1.33 \times 10^{-2}$	$5.33 \times 10^{-2}$	$-6.11 \times 10^{-3}$	$-4.66 \times 10^{-2}$
15	$1.27 \times 10^{-2}$	$1.28 \times 10^{-1}$	$-2.19 \times 10^{-2}$	$-9.03 \times 10^{-2}$

TABLE IX: PV observables for PV  $\pi$ EFT-I and  $\pi$ EFT-II potentials and AV18+UIX strong potential at  $\Lambda = 600$  MeV.

n	$\pi$ EFT-I			$\pi$ EFT-II		
	$a_n^{\gamma(n)}$	$P_\gamma^{(n)}$	$A_d^{\gamma(n)}$	$a_n^{\gamma(n)}$	$P_\gamma^{(n)}$	$A_d^{\gamma(n)}$
1	0.0412	-0.106	-0.153	0.0210	-0.0562	-0.0820
4	-0.0108	0.0103	0.00700	-0.0689	0.0653	0.0434
5	-0.0114	0.0113	0.00812	-0.0644	0.0632	0.0446
6	-0.00362	0.00751	0.0100	-0.0209	0.0447	0.0603
8	0.0151	-0.0163	-0.0133	0.0918	-0.0983	-0.0793
9	0.0100	-0.0126	-0.0123	0.0497	-0.0625	-0.0604
13	0.00934	-0.0207	-0.0283	0.0490	-0.109	-0.149
14	0.00987	-0.0220	-0.0302	0.0271	-0.0836	-0.126
15	0.0170	-0.0379	-0.0518	0.110	-0.244	-0.333

Since all LECs are unknown for each considered case, it is impossible to compare the  $\pi$ EFT-I and the  $\pi$ EFT-II results this time.

#### D. Cutoff and model dependence

The presented results reveal model dependencies of the calculated matrix elements, both on weak as well as on strong interactions. These model dependencies have different levels of importance for calculations of PV effects using different approaches. For the case of the DDH approach, the model dependence is directly related to the reliability of the calculations of PV effects in nuclei. In general, the EFT approach shall lead to model independent results; however, to guarantee a model independence, the intrinsic cutoff dependence must be checked explicitly. For the case of a “hybrid” EFT approach, which is not completely free from the possible model dependencies, a careful analysis of both cutoff dependencies and model dependencies for all matrix elements and for physical observables is required.

In our approach, we used numerically exact solutions for the wave functions of three-nucleon systems, however they depend on the choice of a strong interaction part of the Hamiltonian. For  $M1$  amplitude, we use results of  $N^3LO$  EFT calculations [20] which give a total cross section uncertainty better than 3%, including uncertainties from potential model dependencies, cutoff dependencies and higher order corrections. Another possible source for model dependencies is a choice of PV violating potentials, which, for the EFT approach, means the choice of the scalar functions used for the regularization. It should be noted that in the EFT, the model dependence of physical observables is not directly related to the model dependence of the calculated PV amplitudes because they are affected by the model dependence of the corresponding LECs. Unfortunately, at the present time these LECs are unknown, which prevents us from a derivation of PV observables in EFT formalism.

Since most realistic strong potentials have a similar long range behavior, corresponding to one-pion exchange, the main difference between strong potentials is related to the middle and short range contributions. Thus, rather strong model dependence of PV amplitudes implies that matrix elements related to n-d radiative capture process are sensitive to these short range interactions. This sensitivity to a short range dynamics is new phenomenon observed in radiative n-d capture and is in direct contrast with the case of parity violation in elastic n-d scattering, where PV matrix elements are practically insensitive [15] to the choice of strong potentials.

This is partially related to the fact that in the case of elastic n-d scattering, the dominant contribution to PV effects comes from the  $J = 3/2$  channel, which is repulsive and thus less

sensitive to short range details of the potential. Conversely, in the case of n-d radiative capture, almost all channels equally contribute to the values of PV effects. In addition to that, for the radiative capture, the mechanism of pion exchange is not the dominant one, and, as a consequence, the contributions from heavier meson exchanges (short distance contributions) become important. Therefore, one can see a number of reasons why PV three-body radiative capture processes should be more sensitive to a short distance dynamics than PV effects in three-body elastic scattering. It should be noted that even in the two-body case, circular photon polarization  $P^\gamma$  in n-p radiative capture, which is not dominated by one-pion exchange, shows stronger model dependence [36] than the asymmetry  $a_n^\gamma$ , which defined by the one-pion exchange mechanism.

As mentioned above, a strong dependence of PV effects on the choice of potentials could be a serious problem in the case of the DDH meson exchange model, implying an uncertainty in the theoretical predictions and a difficulty in comparing results of different calculations. On the other hand, in the regular EFT approach, the dependence on a cutoff parameter and on the choice of scalar functions must be absorbed-compensated by the renormalization of the low energy constants. After the proper renormalization one must get a model independent prediction for the low energy observables. This is not exactly true for the hybrid method, where strong interactions are introduced by realistic strong potentials. However, it can be argued that short distance details of the system dynamics would not be very important for the calculations of low energy observables according to the basic principle of the effective field theory. The removal of the possible model dependence, related to the difference in short range parts of the wave functions, can be achieved by the introduction of the cutoff and renormalization of LECs in hybrid approach. A study of the behavior of the calculated matrix elements as a function of cutoff parameters in hybrid approach could be used to check the validity of these arguments.

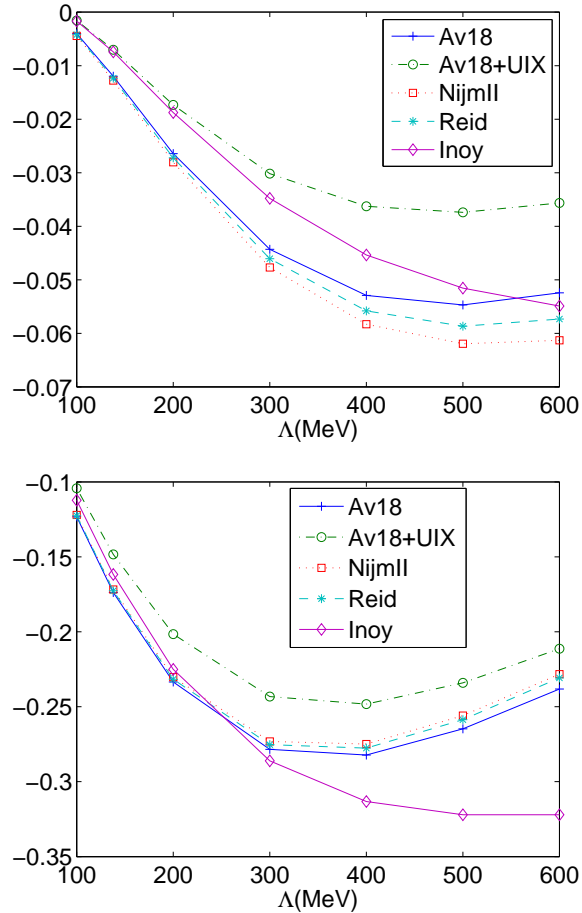


FIG. 1: (Color online) Cutoff and strong model dependencies of the amplitudes for  $\not{n}$ EFT-I calculated with AV18, AV18+UIX, Nijmegen-II, INOY, and Reid strong potentials. The first graph shows  $\mu^2 \tilde{\mathcal{E}}_{\frac{3}{2}(+)}$  for operator 1 and the second graph shows  $\mu^2 \tilde{\mathcal{E}}_{\frac{3}{2}(+)}$  for operator 9 in  $fm^{-\frac{1}{2}}$  units. The multiplier  $\mu^2$  is used to absorb artificial cutoff dependence of  $c_n$  coefficients.

As an example, let us consider the  $\mu^2 \tilde{\mathcal{E}}_{\frac{3}{2}(+)}$  matrix elements as a function of a cutoff mass, which is calculated for operators 1 and 9 in the  $\not{n}$ EFT-I approach with different strong potentials (see Fig.1). The choice of these operators is related to their symmetry properties: the operator 1 has quantum numbers corresponding to pion-exchange while the operator 9 to  $\rho$ -meson exchange. Since we use the same scalar functions both for the  $\not{n}$ EFT-I and for the DDH-II schemes of calculations, we can apply the result of this analysis also to the calculations in the DDH-II scheme by interpreting  $\mu$  as an exchanged meson mass. Once again one observes a rather strong dependence on the choice of a strong potential and on a

cutoff mass parameter.

Analyzing results of Fig.1 from the point of view of the DDH approach, where the matrix element for the operator 1 at  $\mu = m_\pi$  corresponds to the pion-meson exchange and the matrix element for the operator 9 at  $\mu = m_\rho$  corresponds to the rho-meson exchange, one can see a larger strong potential model dependence for the  $\rho$ -meson exchange than for the pion exchange. The observed large difference between AV18 and AV18+UIX calculations at the same  $\mu = m_\rho$  indicates the importance of the inclusion of 3-body strong potentials in the DDH-type model. Unfortunately, most calculations of PV effects in nuclear physics with the DDH potential do not include strong 3-body forces, which could be a possible source for the existing discrepancy [42] in the analysis of PV effects.

On the other hand, from the point of view of the  $\not\equiv$ EFT, the reasonable cutoff mass scale cannot exceed the value of a pion mass, where the dependence on strong interaction potential is small. Since the cutoff in the EFT could be considered as a measure of our knowledge of short range physics, the increasing of the cutoff parameter implies stronger dependence on the short distance details. Fig.1 shows that by lowering the cutoff, one can diminish the strong potential model dependence. This is because by lowering of the cutoff parameter, we are effectively switching to the regime where the theory becomes sensitive only to a long range part of interactions. Then, one can expect a smaller model dependence when the cutoff parameter is low, because all strong potentials have a similar long range behavior. Therefore, Fig.1 is consistent with the basic principle of the EFT and shows that the hybrid method works well.

The remaining weak dependence on a strong interaction model at  $\mu \simeq m_\pi$  scale could be related both to short and to long range parts of the potentials. If they are the remainder of the short distance part of wave function, the difference should be absorbed by LECs. Conversely, the difference in a long range part of the wave function can not be removed by the renormalization of LECs in the hybrid method. However, as demonstrated in [20], this long range part difference is governed by strong interaction observables and should be easily treated by analyzing the correlations between matrix elements and effective range parameters.

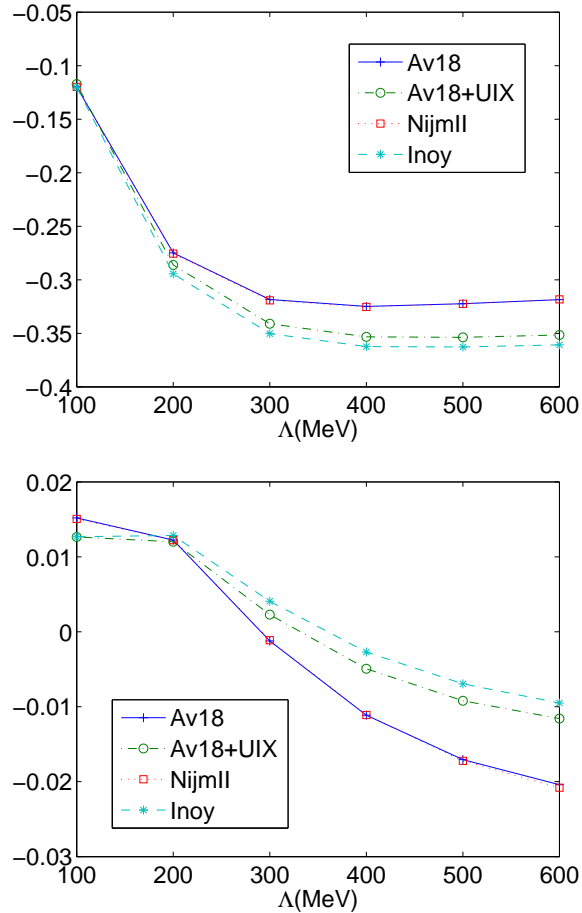


FIG. 2: (Color online) Cutoff and strong model dependencies of the amplitudes for  $\pi$ EFT-I with various strong potential models. The first graph shows  $\Lambda^2 \tilde{\mathcal{E}}_{\frac{1}{2},(+)}$  and the second graph shows  $\Lambda^2 \tilde{\mathcal{E}}_{\frac{3}{2},(+)}$  for op1. in  $fm^{-\frac{1}{2}}$  units. The multiplier  $\Lambda^2$  is used to absorb artificial cutoff dependence of  $c_n$  coefficients.

To analyze the possible model dependence for the pionful EFT approach, let us consider a contribution of operator 1 to  $\Lambda^2 \tilde{\mathcal{E}}_{\frac{1}{2},(-)}$  and to  $\Lambda^2 \tilde{\mathcal{E}}_{\frac{3}{2},(+)}$  calculated in the  $\pi$ EFT-I approach (see Fig. 2). In the  $\pi$ EFT, the physical range for a cutoff mass scale parameter  $\Lambda$  is about  $500 < \Lambda < 800$  MeV. One can observe a rather important dependence on a strong potential model in this region. We cannot discern a long range from a short range model dependency unless all LECs are determined. However, a smaller range of the variation of matrix elements for different strong potentials at the pion mass scale indicates that the contribution of a long range part of strong potentials to the region of the interest ( $500 < \Lambda < 800$  MeV) is small. This means that the large model dependence in this range ( $500 < \Lambda < 800$  MeV) is due to

a short range part of the wave function, therefore, this cutoff and model dependence should be absorbed by the higher order contact terms.

Though the general behavior of the matrix elements is consistent with the expectations of the EFT, the 3-body system is rather complicated to see the direct relations between the 2-body PV potential and 3-body PV matrix elements. Therefore, it is useful to re-analyze the two-body n-p capture process, for which the large model dependence for the circular polarization of photons,  $P^\gamma$ , was reported in [36].

### E. Two body radiative capture( $n + p \rightarrow d + \gamma$ )

Parity violating asymmetry of photons for polarized neutron capture on protons and photon circular polarization for the case of unpolarized neutron capture can be written as

$$a^\gamma = \frac{-\sqrt{2}\text{Re}\{M_1^*(^1S_0)E_1(^3S_1)\}}{|M_1(^1S_0)|^2} \quad (33)$$

$$P^\gamma = \frac{2\text{Re}[M_1(^1S_0)E_1^*(^1S_0)]}{|M_1(^1S_0)|^2}. \quad (34)$$

Here, we neglect  $M_1(^3S_1)$ , and  $E_1(^1P_1 \leftarrow ^3S_1)$  amplitudes. The  $E_1(^3S_1)$  amplitude is a sum of the amplitudes with contributions from parity violating bound state wave function and from parity violating scattering wave ( $^3P_1 \leftarrow ^3S_1$ ). Since  $M_1(^3S_1)$  amplitude is suppressed, one can consider only  $E_1(^1S_0)$  contribution to the  $P^\gamma$ , which is dominated by  $\rho$  and  $\omega$  meson exchanges in the DDH formalism. (The  $a_n^\gamma$  is dominated by one-pion exchange.)

Parity conserving M1 amplitude can be written as

$$M1(^1S_0) = i \frac{\omega\mu_N}{\sqrt{6\pi}\sqrt{4\pi}} \widetilde{\mathcal{M}} = i \frac{\omega\mu_N}{\sqrt{6\pi}\sqrt{4\pi}} \left( \sqrt{4\pi}\sqrt{3}(393.06) fm^{\frac{3}{2}} \right). \quad (35)$$

Then, PV observables can be written as

$$\begin{aligned} a_n^\gamma &= \sum_m \left( \frac{c_m}{\mu_N} \right) (-\sqrt{8\pi}) \frac{\widetilde{\mathcal{E}}^{(m)}(^3S_1)}{\widetilde{\mathcal{M}}(^1S_0)}, \\ P^\gamma &= \sum_m \left( \frac{c_m}{\mu_N} \right) (-2\sqrt{4\pi}) \frac{\widetilde{\mathcal{E}}^{(m)}(^1S_0)}{\widetilde{\mathcal{M}}(^1S_0)}. \end{aligned} \quad (36)$$

Using strong AV18 and weak DDH-II potentials, one can obtain

$$a_n^\gamma = 0.15h_\pi^1 + 0.00137h_\rho^1 - 0.00405h_\omega^1 - 0.00137h_\rho^1, \quad (37)$$

$$P^\gamma = -0.0104h_\rho^0 - 0.00817h_\rho^2 + 0.0111h_\omega^0. \quad (38)$$

TABLE X: Two-body Parity violating observables for potential models with DDH-best parameter values and Bowman's 4-parameter fits.

models	$a_n^\gamma$		$P_\gamma$	
	DDH-best	4-para. fit	DDH-best	4-para. fit
AV18 +DDH-I	$5.25 \times 10^{-8}$	$-4.91 \times 10^{-9}$	$6.94 \times 10^{-9}$	$4.76 \times 10^{-9}$
AV18 +DDH-II	$5.29 \times 10^{-8}$	$-4.81 \times 10^{-9}$	$1.76 \times 10^{-8}$	$3.01 \times 10^{-8}$
NijmII+DDH-II	$5.37 \times 10^{-8}$	$-4.99 \times 10^{-9}$	$2.61 \times 10^{-8}$	$6.41 \times 10^{-8}$
Reid+DDH-II	$5.33 \times 10^{-8}$	$-4.85 \times 10^{-9}$	$2.65 \times 10^{-8}$	$4.68 \times 10^{-8}$
INOY+DDH-II	$5.60 \times 10^{-8}$	$-3.94 \times 10^{-9}$	$2.55 \times 10^{-7}$	$9.68 \times 10^{-7}$

The calculated values of PV observables for different sets of strong potentials and different choices of the DDH coupling constants are summarized in Table X. One can see that the circular polarization  $P_\gamma$ , being dominated by heavy meson exchange, shows large model dependence in agreement with the analysis of n-d case.

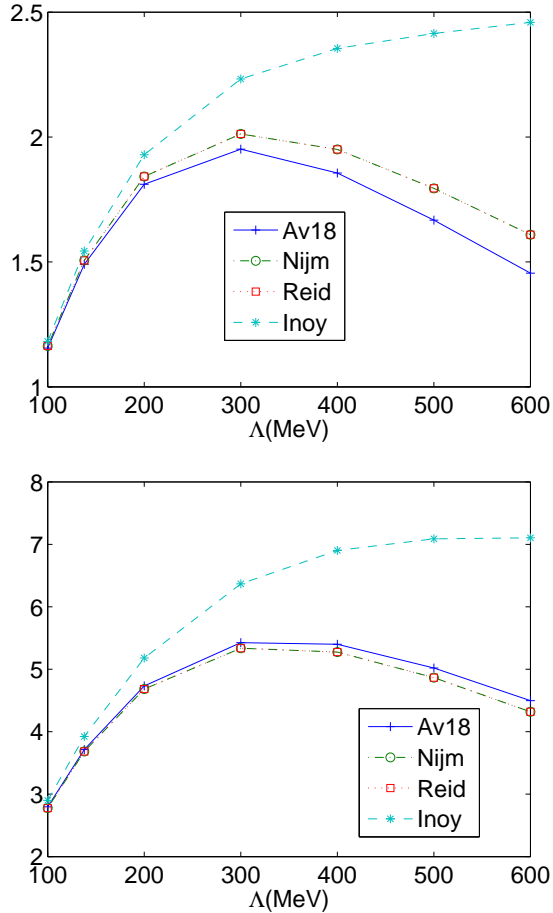


FIG. 3: (Color online) Cutoff and strong model dependencies of amplitudes for  $\pi$ EFT-I with various strong potential models. The first graph shows  $\mu^2 \tilde{\mathcal{E}}_{1,(+)}$  of operator 1 and the second graph shows  $\mu^2 \tilde{\mathcal{E}}_{0,(-)}$  of operator 9 in  $fm^{-\frac{1}{2}}$  units. The multiplier  $\Lambda^2$  is used to absorb artificial cutoff dependence of  $c_n$  coefficients.

The cutoff and model dependence of the transition matrix elements calculated for operators 1 and 9 using the  $\pi$ EFT-I approach, shown in Figure 3, remind the corresponding cutoff and model dependencies of the n-d capture process. One can see that the model dependence is more pronounced at the scale of  $\rho$  or  $\omega$  meson masses in comparison to the pion mass region scale. This is also consistent with the statement given for the hybrid approach that one can regularize the short distance contributions by introducing a cutoff parameter and, as a consequence, reduce the uncertainty related to short range interactions. This indicates that the possible reason for model and cutoff dependencies in the 3-body (n-d capture) pro-

cess has the same origin as those in the 2-body case, and it can be treated regularly in the hybrid approach.

For the completeness of the analysis, we present contributions of different PV operators to PV observables calculated in the  $\not{\pi}$ EFT and the  $\pi$ EFT approaches with AV18 potential (see tables XI and XII, correspondingly). The large difference between matrix elements with pionless and pionful PV potentials could be explained by different scales of the cutoff parameters, and the comparison of the results obtained from these two approaches could be done only after the renormalization of low energy constants.

TABLE XI: Two body Parity violating observables for AV18 and  $\not{\pi}$ EFT potential at  $\mu = 138$  MeV.

n	$\not{\pi}$ EFT-I		$\not{\pi}$ EFT-II	
	$\mu^2 a_n^{(n)}$	$\mu^2 P_\gamma^{(n)}$	$\mu^2 a_n^{(n)}$	$\mu^2 P_\gamma^{(n)}$
1	$6.02 \times 10^{-3}$	0	$1.36 \times 10^{-2}$	0
6	0	$2.48 \times 10^{-2}$	0	$5.71 \times 10^{-2}$
8	0	$1.99 \times 10^{-2}$	0	$1.78 \times 10^{-2}$
9	0	$-2.17 \times 10^{-2}$	0	$-5.97 \times 10^{-2}$

TABLE XII: Two body Parity violating observables for AV18 and  $\pi$ EFT potential at  $\Lambda = 600$  MeV. Only non-vanishing matrix elements are shown.

op	$\pi$ EFT-I	$\pi$ EFT-II	op	$\pi$ EFT-I	$\pi$ EFT-II
	$a_n^{\gamma(n)}$	$a_n^{\gamma(n)}$		$P_\gamma^{(n)}$	$P_\gamma^{(n)}$
1	$1.22 \times 10^{-2}$	$7.14 \times 10^{-3}$	6	$3.05 \times 10^{-3}$	$2.01 \times 10^{-3}$
13	$1.11 \times 10^{-3}$	$5.59 \times 10^{-4}$	8	$2.70 \times 10^{-3}$	$1.80 \times 10^{-3}$
14	$1.33 \times 10^{-3}$	$7.41 \times 10^{-4}$	9	$-4.13 \times 10^{-3}$	$-2.36 \times 10^{-3}$
15	$2.17 \times 10^{-3}$	$1.00 \times 10^{-3}$			

#### IV. CONCLUSION

PV effects in neutron-deuteron radiative capture are calculated for DDH-type and EFT-type, pionless and pionful, weak interaction potentials. Three-body problem was solved

using Faddeev equations in a configuration space, as well as by varying a strong interaction part of the Hamiltonian. A number of different realistic strong potentials have been tested, including AV18 NN interaction in conjunction with UIX 3-nucleon force. The analysis of the obtained results shows that the values of PV amplitudes depend both on the choice of weak and strong interaction models. In order to obtain model independent EFT predictions for PV observables, one should perform all calculations in a self-consistent way [43]. However, we demonstrated that this dependence has the expected behavior in the framework of the standard pionless and pionful EFT approaches even in the "hybrid" approach. Therefore, this dependence is expected to be absorbed by the LECs both in the "hybrid" approach and in the full EFT calculations.

For the case of the DDH approach, the observed model dependence indicates intrinsic difficulty in the description of nuclear PV effects and could be the reason for the observed discrepancies in the nuclear PV data analysis (see, for example [44] and referencies therein). Thus, the DDH approach could be a reasonable approach for the parametrization and for the analysis of PV effects only if exactly the same strong and weak potentials are used in calculating all PV observables in all nuclei. However, the existing calculations of nuclear PV effects have been done using different potentials; therefore, strictly speaking, one cannot compare the existing results of these calculations among themselves. Further, most of the existing calculations do not include three body interactions which is shown to be important.

We would like to mention that the observed sensitivity of PV effects to short range parts of interactions could be used as a new method for the study of short ranges nuclear forces. Once the theory of PV effects is well understood, or once we use exactly the same parametrization for weak interactions, PV effects can be used to probe a short distance dynamics of different nuclear systems described by different strong potentials.

### **Acknowledgments**

This work was supported by the DOE DE-FG02-09ER41621 and NSF PHY-0758114 grants. This work was granted access to the HPC resources of IDRIS under the allocation 2009-i2009056006 made by GENCI (Grand Equipement National de Calcul Intensif). We

thank the staff members of the IDRIS for their constant help.

- 
- [1] S.-L. Zhu, C. M. Maekawa, B. R. Holstein, M. J. Ramsey-Musolf, and U. van Kolck, Nucl. Phys. **A748**, 435 (2005).
  - [2] B. Holstein, *Neutrons and hadronic parity violation* (2005), proc. of Int. Workshop on Theoretical Problems in Fundamental Neutron Physics, October 14-15, 2005, Columbia, SC, <http://www.physics.sc.edu/TPFNP/Talks/Program.html>.
  - [3] B. Desplanque, *Weak couplings: a few remarks* (2005), proc. of Int. Workshop on Theoretical Problems in Fundamental Neutron Physics, October 14-15, 2005, Columbia, SC, <http://www.physics.sc.edu/TPFNP/Talks/Program.html>.
  - [4] M. J. Ramsey-Musolf and S. A. Page, Ann. Rev. Nucl. Part. Sci. **56**, 1 (2006).
  - [5] B. Desplanques, J. F. Donoghue, and B. R. Holstein, Annals of Physics **124**, 449 (1980).
  - [6] C. P. Liu, Phys. Rev. **C75**, 065501 (2007).
  - [7] L. Girlanda, Phys. Rev. **C77**, 067001 (2008), 0804.0772.
  - [8] D. R. Phillips, M. R. Schindler, and R. P. Springer, Nucl. Phys. **A822**, 1 (2009).
  - [9] J. W. Shin, S. Ando, and C. H. Hyun, Phys. Rev. **C81**, 055501 (2010).
  - [10] M. R. Schindler and R. P. Springer (2009), 0907.5358.
  - [11] O. P. Sushkov and V. V. Flambaum, Sov. Phys. Usp. **25**, 1 (1982).
  - [12] V. E. Bunakov and V. P. Gudkov, Nucl. Phys. **A401**, 93 (1983).
  - [13] V. P. Gudkov, Phys. Rept. **212**, 77 (1992).
  - [14] R. Schiavilla, M. Viviani, L. Girlanda, A. Kievsky, and L. E. Marcucci, Phys. Rev. **C78**, 014002 (2008).
  - [15] Y.-H. Song, R. Lazauskas, and V. Gudkov, Phys.Rev. **C83**, 015501 (2011), 1011.2221.
  - [16] A. Moskalev, Sov. J. of Nucl. Phys. **9**, 99 (1969).
  - [17] E. H. E. Hadjimichael and V. Newton, Nucl. Phys. **A228**, 1 (1974).
  - [18] B. H. McKellar, Phys.Rev. **C9**, 1790 (1974).
  - [19] B. Desplanques and J. Benayoun, Nucl.Phys. **A458**, 689 (1986).
  - [20] Y.-H. Song, R. Lazauskas, and T.-S. Park, Phys. Rev. **C79**, 064002 (2009).
  - [21] S. Pastore, L. Girlanda, R. Schiavilla, M. Viviani, and R. B. Wiringa, Phys. Rev. **C80**, 034004 (2009).

- [22] V. G. J. S. R. B. Wiringa and R. Schiavilla, **C51**, 38 (1995).
- [23] Z. P. P. Doleschall, I. Borbely and W. Plessas, Phys. Rev. **C67**, 064005 (2003).
- [24] V. G. J. Stoks, R. A. M. Klomp, C. P. F. Terheggen, and J. J. de Swart, Phys. Rev. C **49**, 2950 (1994).
- [25] J. C. B. S. Pudliner, V. R. Pandharipande and R. B. Wiringa, Phys. Rev. Lett. **74**, 4396 (1995).
- [26] S. Weinberg, Phys. Lett. **B251**, 288 (1990).
- [27] S. Weinberg, Nucl. Phys. **B363**, 3 (1991).
- [28] Y.-H. Song, R. Lazauskas, T.-S. Park, and D.-P. Min, Phys. Lett. **B656**, 174 (2007).
- [29] R. Lazauskas, Y.-H. Song, and T.-S. Park (2009), 0905.3119.
- [30] T. S. Park et al., Phys. Rev. **C67**, 055206 (2003).
- [31] L. Girlanda et al. (2010), 1008.0356.
- [32] Y.-H. Song, R. Lazauskas, and V. Gudkov, Phys.Rev. **C83**, 065503 (2011), 1104.3051.
- [33] Y.-H. Song, R. Lazauskas, and V. Gudkov, Phys.Rev. **C84**, 025501 (2011), 1105.1327.
- [34] H. W. Griesshammer, M. R. Schindler, and R. P. Springer, Eur.Phys.J. **A48**, 7 (2012), 1109.5667.
- [35] B. Desplanques, J. F. Donoghue, and B. R. Holstein, Ann. Phys. **124**, 449 (1980), ISSN 0003-4916.
- [36] R. Schiavilla, J. Carlson, and M. W. Paris, Phys. Rev. **C70**, 044007 (2004).
- [37] C. Hyun, S. Ando, and B. Desplanques, Eur.Phys.J. **A32**, 513 (2007), nucl-th/0609015.
- [38] L. D. Faddeev, Sov. Phys. JETP **12**, 1014 (1961).
- [39] R. Lazauskas (2003), universite Joseph Fourier, Grenoble.
- [40] R. Lazauskas, Few-Body Systems **46**, 37 (2009), URL <http://arxiv.org/abs/0808.1650>.
- [41] J. D. Bowman, “Hadronic Weak Interaction”, INT Workshop on Electric Dipole Moments and CP Violations, March 19-23, 2007, [http://www.int.washington.edu/talks/WorkShops/int\\_07\\_1/](http://www.int.washington.edu/talks/WorkShops/int_07_1/).
- [42] B. R. Holstein, Fizika. **B14**, 165 (2005), nucl-th/0607038.
- [43] V. Gudkov and Y.-H. Song, Phys. Rev. **C82**, 028502 (2010).
- [44] B. R. Holstein, Eur. Phys. J. **A41**, 279 (2009).